UDC 532.516:536.24.01

A. KHALATOV[1], A. BYERLEY[2]

[1]Institute for Engineering Thermophysics, National Academy of Sciences, Kiev, Ukraine
[2]United States Air Force Academy, Colorado Springs CO, USA

UNSTEADY FLOW STRUCTURE: DUAL ARRAY OF SPHERICAL AND CYLINDRICAL DIMPLES

Виконано експериментальну програму у Військово-повітряній академії США, скеровану на вивчення нестаціонарної структури потоку попереду, всередині та за подвійним рядом дрібних (h/D = 0,1) сферичних та циліндричних заглиблень на плоскій поверхні. Порівняння показало, що перший ряд заглиблень "пригнічує" флуктуації другого ряду.

Выполнена экспериментальная программа в Военно-воздушной академии США, направленная на изучение нестационарной структуры потока перед, внутри и за двойным рядом "мелких" (h/D = 0,1) сферических и цилиндрических углублений на плоской поверхности. Сравнение показало, что первый ряд углублений "подавляет" флуктуации второго ряда.

The experimental program was performed in the U.S. Air Force Academy to obtain details of the unsteady flow structure in front, within and downstream of a dual array of shallow (h/D = 0.1) spherical and cylindrical dimples on a flat plate. Comparisons have shown that the first row "suppresses" fluctuations of the second row.

D – dimple projected (surface) diameter, m;
f – frequency of bulk flow oscillations, s^{-1};
h – dimple depth, m;
H* – channel height, m;
L – extent of in-dimple separation zone, m;
Re_D – diameter based Reynolds number, $U_\infty D/\nu$;
Re_x – axial distance Reynolds number, $U_\infty x/\nu$
S_x, S_z – axial and spanwise dimple pitch, m
Sh – Strouhal number, $f \cdot D/U_\infty$
x – axial distance from the leading edge, m;
U_∞ – approaching flow speed, m/s;
z – spanwise distance, m.

Greek symbols:

δ – boundary layer thickness, m;
ν – kinematic viscosity, m^2/s.

Subscripts:

o – pre-dimple flow parameters.

OBJECTIVE

As reported in [1, 2], the suction side of gas turbine blade suffers from the boundary layer separation when operating at the off-design conditions. The separation and increase in the blade profile losses cause a significant reduction in the turbine efficiency. To guard against this, both active and passive flow control techniques are considered. Compared with other passive techniques (V-grooves; wires), the shallow spherical dimples have demonstrated the best results in terms of reduction in separation losses and improvements in the region of a flow reattachment [1, 2].

There is a vast experimental and theoretical database in the literature involving a single dimple on a flat wall and multiple dimples in the rectangular channel. The author refers reader to the extensive reviews given by Ligrani, et al. [3] and Khalatov [4]. However the application of dimples for the flow separation control over turbine blade requires fundamental knowledge of the fluid flow features for single- or dual array of dimples at relatively low flow velocity regimes. For the single array of shallow dimples (h/D = 0.10) the limited fluid flow database has been presented by Lake, et al. [1], Rouser [2] (spherical dimples/turbine blade) and Khalatov, et al. [5] (spherical and cylindrical dimples/flat plate). There was no data revealed for the dual array of dimples; as supposed this configuration provides better wall coverage due to the downstream overlapping of wakes.

The objective of this study is to investigate the details of unsteady flow features in front, inside and downstream of a dual array of shallow (h/D = 0.10) dimples on a flat plate. The experimental program was performed at relatively low Reynolds number conditions ($Re_D < 25{,}000$) using the dye flow visuali-

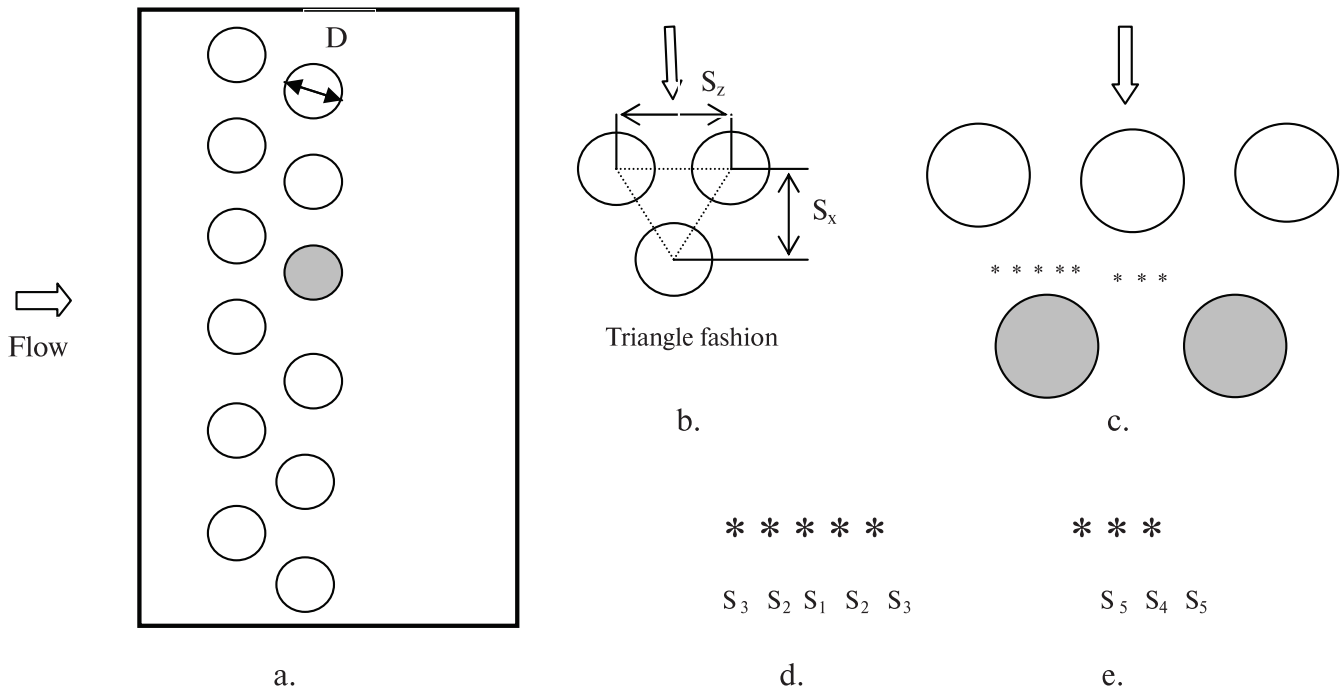

Figure 1. Dual array of dimples in the staggered mode (no dye ports shown inside the dimple).

zation technique. This includes a laminar flow in front of the first row, but both laminar and turbulent flow in front of the second row. The shallow dimples were taken for the experimentation as providing reduced additional pressure losses. Both spherical and cylindrical dimple configurations were tested to assess their relative characteristics.

EXPERIMENTAL FACILITY

Test section

The experimental program was performed in the U.S. Air Force Academy (Colorado Springs) closed-circuit water tunnel described by Khalatov, et. al [5]. The water tunnel is capable of operating over a speed range of 0.07 to 0.52 m/s. The inlet nozzle has a contraction ratio of 6:1; the mean velocity at the inlet is uniform to within ± 2%, the mean flow angularity is within ± 1.0 degrees in both pitch and yaw directions.

The test channel is 1,830 mm long with a rectangular cross section (610 mm height; 457 mm width). The sidewalls and floor (bottom) were made of a glass to allow access for flow observations. The test section (Fig.1) is an acrylic flat plate with an elliptically shaped leading edge. It is 19 mm thick, 1,220 mm long and 381 mm wide.

A dual array of dimples (Fig.1a) was machined in the test section in the staggered mode using the isosceles triangle fashion (Fig.1b). The dimple (spherical and cylindrical) projected (surface) diameter is 50.8 mm, the depth is 5.08 mm providing the shallow dimple configuration (h/D = 0.1). The center of the first row locates at 88 mm from the plate leading edge to avoid the effect of pre-dimple boundary layer thickness. For the first and second rows the spanwise pitch is 76.2 mm (S_z/D = 1.5), the axial pitch between first and second rows is 88.0 mm (S_x/D = 1.73). Such a configuration provides overlapping of wakes (25%) after the dual array of dimples and much better surface coverage.

The dimpled flat plate in the test section was suspended upside down, so the flow structures could be observed through the transparent (glass) floor with the aid of an inclined mirror placed below the test channel. To visualize the flow structures, five different colors of dye were injected through five cylindrical ports in front of the representative dimple (Fig. 1c, 1d) and inside it. Additional three ports were made between adjacent cylindrical dimples of the second row (Fig. 1c, 1e).

A digital camcorder SONY-DCR VX2000 was used to record the unsteady flow patterns. The video images were stored as digital (AVI) files to allow com-

puter screening at a reduced frame rate (slow motion) with Adobe Premiere 6.5 Software. In this way, the flow structures and patterns could be carefully observed, analyzed and characterized. From this data the frequency of the bulk flow oscillations was determined by counting the number of fluctuations shed by the dimple during a 15 sec interval [5].

The Reynolds number Re_D ranged from 3,260 to 23,450, corresponding to a range of Reynolds numbers Re_x in front of the first array from 4,010 to 28,840. The laminar flow kept in front of the first array of dimples, the non-dimensional boundary layer thickness δ_0/h varied from 0.3 to 0.4.

Uncertainty Analysis

Velocity measurements were calibrated to within ± 1.8% using a video camera to record the time for a volume of dye to go the length of the test section (video camera frame rate is 29.97 frames per second). The uncertainty in Reynolds number was estimated to be within ± 2.4%. The uncertainty in frequency was estimated to be ± 10.6%, which contributed to an uncertainty in the Strouhal number of ± 10.9%. At lower free-stream velocities, both the frequency of fluctuations and the Strouhal number were as low as ± 3.66% and ± 4.35%, respectively. All uncertainty estimates are based upon the methods of Coleman and Steele [6].

DUAL ARRAY OF CYLINDRICAL DIMPLES

A description of the flow patterns inside and downstream of a single array of cylindrical dimples has been considered in [5]. As concluded, the adjacent dimples strongly influence the flow patterns and downstream bulk flow fluctuations. At low Reynolds numbers, the frequency of bulk flow fluctuations are close to that obtained for a single dimple, although between Re_D = 8,000 and Re_D = 10,400 the Strouhal number drops below that for a single dimple.

Dye injection in front of and within a dimple

The experimental runs were conducted across the range of the water velocities from 0.072 to 0.52 m/s corresponding with diameter-based Reynolds numbers Re_D ranging from 3,265 to 23,450. The non-dimensional boundary layer thickness δ_0/h in front of the first row was 0.40 at Re_D = 5,220 and 0.28 – at Re_D = 16,240. Five different dye colors were injected through five cylindrical ports machined both upstream (S_1 –, S_2 –, S_3 – streamlines; Fig. 1c, 1d) and inside (not shown) representative dimple.

The central S1-streamline in the space between the first row adjacent dimples revealed a laminar flow structure in front of the second row in the whole range of Reynolds number (up to Re_D = 23,450). At $Re_D \le 4{,}170$ both S_2 – streamlines were almost parallel to each other, while S_3 – streamlines located in the wake of the first array experienced weak fluctuations. Fluctuations of S_2 – streamlines observed only at $Re_D > 5000$ (Fig.2a), with the laminar-turbulent flow transition (streamline destruction) completed by Re_D = 12,250. On both S_3 – streamlines the turbulence indicated at Re_D = 5,260.

Inside a dimple, the flow began to separate at $Re_D > 5{,}260$, the extent of the separated flow area was increased with growth of the Reynolds number. At Re_D = 6,800 a weak flow rotation occurred inside the dimple with a small flow fluctuations zone near the back dimple rim. This might be due to the flow instability inside a dimple. After Re_D = 9,200 the in-dimple separation zone is almost symmetrical. Moreover, due to the laminar-turbulent flow transition after the first row (S_2 – and S_3 – streamlines at Re_D >12,250) the separation zone extent remains approximately constant at around 50% of the dimple area up to Re_D = 23,450. Unlike this, for the single array of dimples a separation zone extent increased monotonically with the Reynolds number growth [5].

Downstream of a dimple the flow exhibits a “strip” pattern (Fig. 2b) at $Re_D \le 4{,}170$, while at Re_D = 5,260 the flow transitioned to the turbulent flow (Fig. 2a). The highly-developed downstream bulk flow fluctuations were observed at $Re_D > 5{,}260$.

Dye injection between dimples

The flow structure between adjacent dimples of the second array was visualized to study the flow pattern after the dimple in the first array. Three cylindrical ports (Fig. 1c; 1e) were located at the distance of 30 mm downstream of the dimple back edge.

Since this distance is very small (≈0.60·D), the first row heavily influenced the flow structure. At $Re_D < 5{,}260$ the flow kept the laminar structure with weak flow fluctuations of the S_4– streamline. Both S_5– streamlines demonstrated significant spanwise

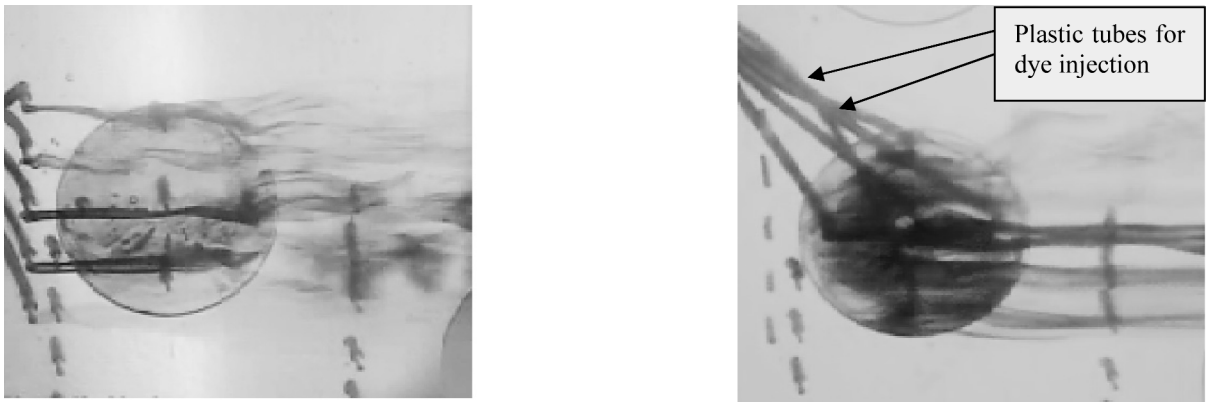

a *b*

Figure 2. Dual array of cylindrical dimples (second row). a: Re_D = 5,260. b: Re_D = 4,170. Dye injection in front of (a) and inside a dimple (b).

fluctuations. Based on the observations of dye behavior, the conclusion was made that the turbulence on the S_5 – streamline started at Re_D = 6,850, while on both S_4 – streamlines – at Re_D = 8,140. For a single array of cylindrical dimple the downstream laminar-turbulent flow transition began at Re_D = 6,670 [5]. This value of the critical Reynolds number is close to that obtained for S_3 –, S_4 – and S_5 – streamlines.

At Re_D > 9,300, both S_5 – streamlines moved in towards the second array, however at Re_D>15,000 the streamlines were fully "sucked" into the dimple area. This is a clear evidence of the cross flow talking between dimples located in the first and second array.

Laminar – turbulent flow transition

The experimental results considered above led to the following primary conclusions:

- At Re_D < 5,260 the flow structure is the laminar one throughout the flow area.
- In the area between Re_D = 5,260 and Re_D = 12,250, the flow between adjacent dimples of the first row is laminar, but is turbulent beyond the dimple in the first row. After the second array it is the fully developed turbulent flow.
- At Re_D > 12,250 the flow was the turbulent one throughout the flow area.
- Flow conditions in front of a dimple influence weakly the critical Reynolds number after a dimple. Beyond a single array the flow became turbulent at Re_D > 6,670 (laminar flow in front of), while beyond a double array – at Re_D> 5,260 (laminar flow accompanied with a wake from the first array dimple; greater boundary layer thickness).

Bulk flow fluctuations

The correlation Sh = f (Re_D), describing the bulk flow fluctuations downstream of the dimple in the second array is shown in Fig.3. For the single and double arrays the correlation Sh = f (Re_D) is a curve with a maximum at a certain Reynolds number (Remax). Therefore, at Re < Re_{max} the growth of frequencies of flow fluctuations dominated over the water velocity growth, and vice versa at Re < Re_{max}. For the single array, the correlation Sh = f (Re_D) reaches a maximum at $Re_D \approx$ 10,200, while for the double array – at $Re_D \approx$ 10,000. However the single array has a sharp peak in the Strouhal number curve, while the double array – a much broader peak.

Unlike the single row, the flow fluctuations beyond a second row did not occur at Re_D < 3,000. As a whole, the fluctuations generated by the second row were lower than those generated by the single row. This is due to the complex flow structure, transition to the turbulent flow and greater boundary layer thickness in front of the dimple, as well as lower in-dimple separation zone extent. At Re_D>20,000, flow fluctuations (Strouhal number) for both configurations are actually identical, therefore no influence of the upstream flow structure occurred in this Reynolds number regime.

As reported, the double array provided the downstream laminar-turbulent flow transition at Re_D > 5,260, while in the space between dimples – at Re_D > 8,140.

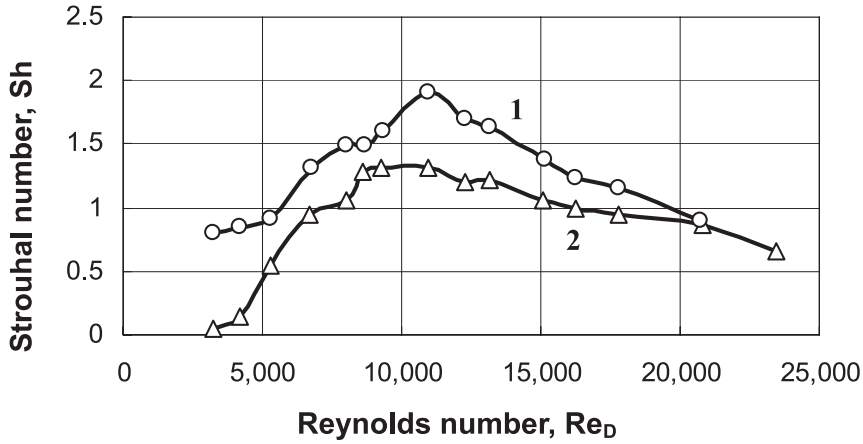

Figure 3. Bulk flow fluctuations: single (1) and dual (2) array of cylindrical dimples.

The single array provided transition after a dimple at $Re_D > 6{,}670$ with laminar flow between adjacent dimples. Therefore, at $Re_D > 8{,}140$ the double array generated the downstream turbulent flow throughout the flow field. This important fact can be employed in design of the flow separation control devices.

DUAL ARRAY OF SPHERICAL DIMPLES

Description of the flow patterns for a single array of spherical dimples has been considered in [5]. As found, across the whole range of Reynolds number the Strouhal number is approximately 10% greater than for a single dimple. However for both configurations the "peak" of the Strouhal number curve was occurred at $Re_D \approx 16{,}300$.

Dye injection in front of and within a dimple

The experimental program was performed across the same range of fluid boundary conditions as for the dual array of cylindrical dimples.

At low flow velocities ($Re_D = 3{,}310$) the S_1– streamline over a dimple was parallel to the axial flow direction, while S_2 – and S_3 – streamlines demonstrated weak spanwise fluctuations. At $Re_D > 10{,}500$, the streamlines over the dimple experienced substantial spanwise fluctuations, especially noticeable in the dimple axis area. At higher flow velocities ($Re_D > 12{,}250$) the streamlines were twisted and broken.

Inside a dimple the unsteady flow pattern appeared at $Re_D = 5{,}500$ with periodic downstream bulk flow fluctuations. At higher flow velocities, these fluctuations increased, so the bulk flow fluctuations were almost regular at $Re_D = 7{,}940$. At $Re_D = 9{,}480$ the asymmetric twin vortex action began inside the dimple, which transformed into a symmetrical twin vortex pair at $Re_D = 12{,}250$ occupying around 50% of the dimple area. At $Re_D = 17{,}050$ the twin vortex pair started to dissipate into the chaotic streamline patterns. This chaos increased with increases in flow velocity leading to a fully chaotic flow in upstream dimple area. At $Re_D = 23{,}450$ the in-dimple separation zone extent was around 70%.

Downstream of a dimple, the streamlines fluctuated in the spanwise direction; increasing the flow velocity led to the growth of spanwise fluctuations and transition to turbulent flow at $Re_D = 9{,}480$.

Laminar-turbulent flow transition

Results given above show that S_1– and S_2 – streamlines in front of the dimple kept the laminar flow pattern up to $Re_D = 23{,}450$, while S_3 – streamline demonstrated transition to the turbulent flow at $Re_D > 9{,}480$. Turbulence and a wide wake downstream of a dimple was detected at $Re_D > 9{,}480$. This transition links with the asymmetric flow pattern inside a dimple. As far as the single dimple and single row of dimples is concerned, the flow transition after dimple(s) occurred at $Re_D > 7{,}940...7{,}980$ [5].

Bulk flow fluctuations

The correlation $Sh = f(Re_D)$, demonstrating the bulk flow fluctuations downstream of the single- and double array of spherical dimples is presented in Fig.4. Again, this correlation is a curve with a maximum at a certain Reynolds number (Remax). In both

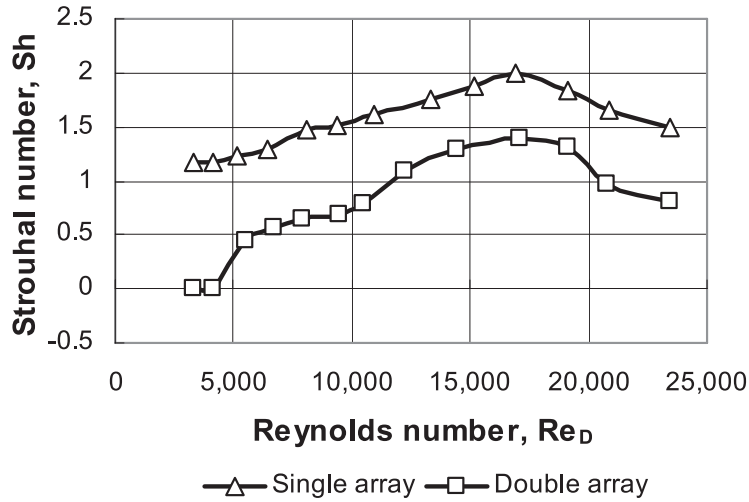

Figure 4. Bulk flow fluctuations: spherical dimples.

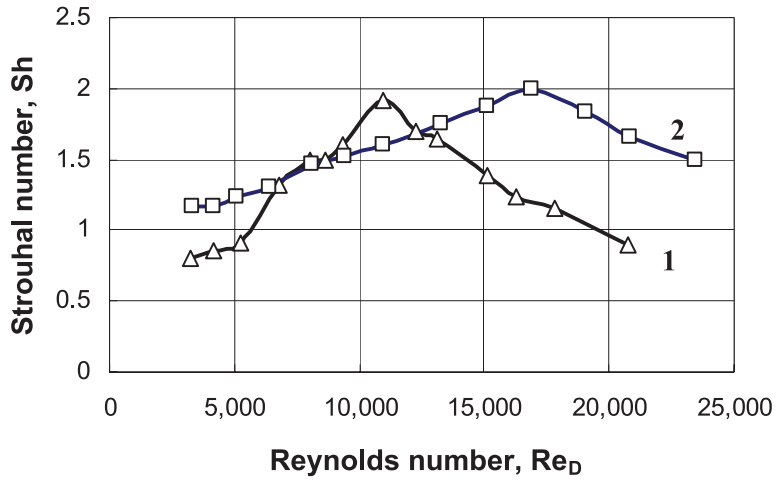

Figure 5. Comparisons: bulk flow fluctuations downstream of a single array of dimples. 1 – cylindrical dimples. 2 – spherical dimples.

cases, the curve Sh = f(Re_D) reached a maximum at Re_D17,200. The broader "peak" in the Strouhal number curve can be explained by the "smooth" shape of the spherical dimple. As for the cylindrical case, the frequencies for the double row are less than for the single row, particularly at Re_D< 15000. The reduction for the spherical dimple case actually looks greater than for the cylindrical dimple case shown in Fig.3. Unlike the single array, the flow fluctuations beyond a second array did not appear at Re_D < 4,500.

COMPARISONS

A comparison of the bulk flow fluctuation frequencies generated by the cylindrical and spherical dimples in the single-row mode is presented in Fig.5. For both configurations, the magnitude of Strouhal number maximum is approximately the same, however for the spherical dimple this maximum occurs at a greater Reynolds number. At Re_D < 7,500 and Re_D > 12,500 the spherical dimple generates more significant bulk flow fluctuations.

Bulk flow fluctuations generated by the second row are given in Fig.6. At Re_D numbers ranging from 5,000 to 13,000, the fluctuation frequencies of the cylindrical dimples exceeded those for spherical dimples. However, at Re_D > 20,000 there was no effect of the dimple shape on the magnitude of the Strouhal number. For both configurations, the maximum value of Strouhal number is approximately the same.

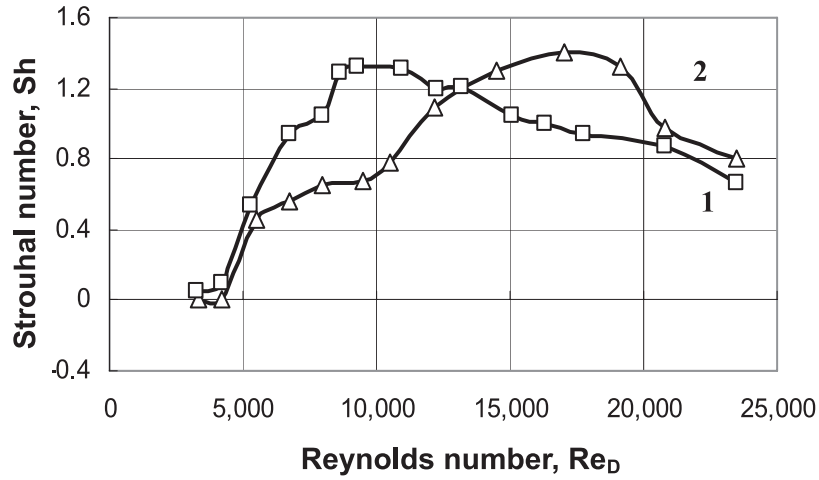

Figure 6. Comparisons: bulk flow fluctuations downstream of a dual array of dimples. 1 – cylindrical dimples. 2 – spherical dimples.

CONCLUSIONS

For the dual and single array the dimple shape (spherical/cylindrical) plays important role in the level of downstream bulk flow fluctuations. For the spherical dimple the "peak" in the curve $Sh = f(Re_D)$ is broader than that for the cylindrical dimple. The upstream vortex structures reduce bulk flow fluctuations after the second row making them smaller than those after the single.

According to visual flow observations transition to the turbulent flow after cylindrical dimples occurred at Re_D= 5,260, while beyond spherical dimple – at Re_D= 9,480. As follows (Fig. 6), for both configurations this transition corresponds to the "narrow" range of Strouhal number from 0.6 to 0.7.

ACKNOWLEDGMENTS

This research was performed while visit of Prof. A Khalatov to the Aeronautics Laboratory of U.S. Air Force Academy in Colorado Springs (U.S. National Research Council Grant). The partial support of CRDF Grant # UE2-552-KV-02 is also acknowledged.

REFERENCES

1. *Lake J.P., King, P.I., Rivir R.B.* Low Reynolds Number Loss Reduction on Turbine Blades with Dimples and V-Grooves // AIAA Paper № 00-738. – 2000.

2. *Rouser K.* Use of Dimples to Suppress Boundary Layer Separation on a Low Pressure Turbine Blade. – M.S. Thesis. – Air Force Institute of Technology. WPAFB, Ohio, USA. – 2002.

3. *Ligrani P.M., Oliveira M.M Blaskovich, T.* Comparison of Heat Augmentation Techniques // AIAA Journal. – Vol.41. – №3. – 2003. – pp.337-362.

4. *Khalatov A., Borisov I., Shevtsov S.* Heat Transfer and Hydrodynamics in Centrifugal Fields. Volume 5: Heat and Mass Transfer, Thermal-hydraulic Performance of Vortex and Swirling Flows. – Kiev: National Academy of Sciences of Ukraine. –2005. – 500p. (in Russian).

5. *Khalatov A., Byerley A., Seong-Ki Min, Ochoa D.* Flow Characteristics Within and Downstream of Spherical and Cylindrical Dimple on a Flat Plate at Low Reynolds Numbers // ASME Paper №GT2004 – 53656. – 2004.

6. *Coleman H. Steele G.* Experimentation and Uncertainty Analysis for Engineers. – John Wiley & Sons. New York, NY. 2d Edition, – 1999. – 275p.

Получено 13.07.2006 г.